A New Technique for Geometry Based Visual Depth Estimation for Uncalibrated Camera

Ibrar Ullah Jan[#1], Dr. Naeem Iqbal[*2]

[#]*Department of Electrical Engineering, Pakistan Institute of Engineering and Applied Sciences(PIEAS) Nilore, Islamabad, Pakistan.*

[1]ibrar1976@hotmail.com

[*] *Department of Electrical Engineering, Pakistan Institute of Engineering and Applied Sciences(PIEAS) Nilore, Islamabad, Pakistan.*

[2]naeem@pieas.edu.pk

***Abstract*— The most challenging issue in the field of visual control system is the accurate estimation of depth upon which all other parameters of pose estimation may depend. Here we have introduced a new approach for the depth estimation problem of a visual control system with a moving camera and stationary target. A unique visual pattern is designed to achieve the desired depth of the vision based system. In this paper the unknown depths of the special geometrical feature points are estimated from the pre-calculated depth calibrated equations, whose affects are then combined to acquire the desired goal. This specialized technique doesn't require any conventional camera calibration parameters (e.g., camera intrinsic parameters); rather it works on the specialized and accurate depth calculating calibration equations described in this paper. Simulation and experimental applications are presented which verify the performance of the proposed technique. The vision system (i.e., a wireless camera, pointing downwards) is mounted with a mechanical assembly which can move laterally as well as up and down. The required algorithm is designed in MATLAB.**

***Keywords*— Geometry, Vision system, Lateral position, Depth estimation, Specialized depth calculating calibrated equations.**

Introduction

I. INTRODUCTION

Accurate visual depth estimation is a challenging problem but an important task in the field of vision based control system and aerial robotics. The applications of the applied technique can be extended to un-manned aerial vehicles (UAVs) to achieve high level of autonomy [1]. Similarly the addition of visual sensors to the systems [2] and [5] can make the control system more reliable for practical applications. The sensing schemes for depth control system can be mainly summarized in two categories: visual sensor (cameras) only, or a combination of multiple sensors. Our sensing strategy belongs to vision-only system. With recent development in camera technology and image processing hardware, it is natural to consider a vision-based solution to the problem of aerial robotics. The estimation of depth from image sequence using a known camera motion is important in a variety of applications of computer vision applied to robot navigation and manipulation. The algorithm designed for such estimation can be based on an online incremental fashion.

Relating with the previous work on such systems, we studied [1]. The developed system is using vision and global positioning based autonomous landing of a helicopter on stationary target. Some of the assumptions were derived from here. The image processing section described in this paper is derived from [3] and [4] and Image processing Toolbox of MATLAB7.1. All ego motion compensation techniques attempt to make an estimate of the camera motion according to some transformation model. While perfect estimates of camera ego motion can only be realized with highly non-linear and unwieldy models, robust results are achieved using simpler techniques. [6] Uses affine formulation based on the assumption that the distance from the observer to the targets is large compared to the depth of the scene. Some applications, though, require slightly more complex bilinear models [7]. In contrast with the previous work mentioned in the references, we have developed a control strategy that allows the camera to achieve its desire position and depth. The control system is based only on the images received and decisions are taken according to the reference and actual visual states of the camera. This allows the system to have virtual feedback link between the camera and the controlling computer. As the system is hardware-independent, it is very flexible and changes can be made according to the actual parameters of the hardware system under consideration. Another better aspect of this system is that we can easily add other future ideas according to our wishes to make the system more reliable, accurate and safe for a particular application. It is important to mention here that we use a USB based I/O card and other switching and signal conversion electronics for interfacing the controller (computer) and the mechanical setup again connected through a wireless system. The mechanical system has a combination of three DC motors connected with three separate channel of a three-channel receiver. The corresponding three-channel transmitter is interfaced with the output of the USB I/O card. The inputs to the USB card are directly controlled by the designed algorithms which take decisions purely on the image processing system. The general system block diagram is shown in Fig. 1. The broken arrows show the wireless connections.

978-1-4244-3986-7/09/$25.00

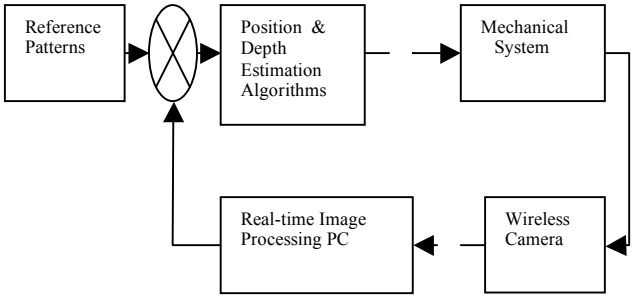

Fig. 1 General Block Diagram

Also the general flow diagram of the system is shown in Fig. 2. The paper is organized as follows. In section 2, we describe an introduction to the experimental setup and the assumptions we have included. Section 3, presents the general steps involved in the image processing. Section 4, describes the technique used to find the pre-defined depth estimation calibration equations. In section 5, we have mentioned the simulation and experimental results. Finally, we have added conclusion and future work in section 6.

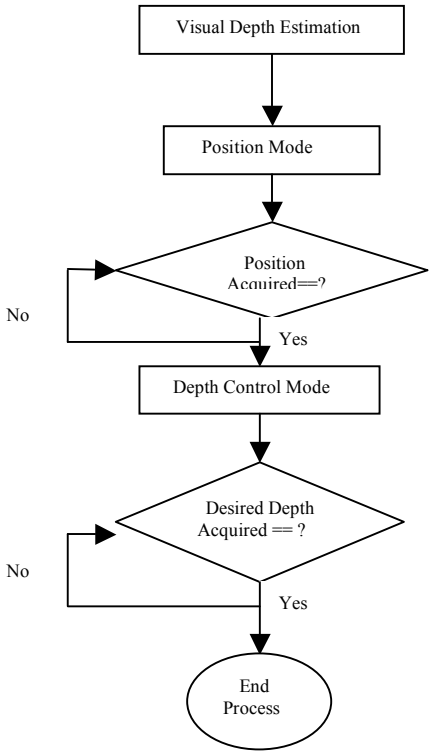

Fig. 2 Flow Diagram

II. EXPERIMENTAL SETUP WITH ASSUMPTIONS

Real-time processed images are received from the wireless camera through its receiver and compared with the reference patterns into the computer. Based on the results produced by the comparison the computer controller generates control commands which are sent to the USB I/O card for interfacing with the real world. The outputs produced from this card in response are further processed by 'Signal Conversion Electronics' to make it suitable for the three-channel transmitter. This part of the system has some automatic control switching mechanism so that we can easily switch among the three channel of the transmitter. The receiver on the other side attached to the mechanical assembly responds to these signals and operate the corresponding DC motors which forces the camera to the desired direction. The Three motors are responsible for the three translation movements of the camera individually. The wireless camera attached to the mechanical system captures images according to the actual status of the camera and transmits it to its receiver. The dashed arrows in the diagram show the wireless communication system. The feedback system is not connected through direct hardware, so we call it a virtual feedback system. Next we include the following assumptions to our system

1) The vibrations in the mechanical assembly are negligible.
2) The principal axis of the camera is aligned with that of mechanical assembly [2], when it is perfectly horizontal.
3) The camera is perpendicular to the ground plane and pointing downwards [2].
4) The ground (here the surface on which the pattern is made) is plane.
5) The target pattern and intensity levels are different from the background.
6) The size of the target pattern in the image plane is much smaller than the image size.
7) There are no rotational movements of the camera.

The first and second assumptions affect the accuracy of the control process. The third and fourth assumptions avoid the possibility that the camera can view the landing area through an angle. Further, to precisely differentiate the target from the background and to avoid the possibility that vision system can detect a wrong pattern to be a true one, we have added the fifth assumption. The sixth and seventh assumptions again affect the accuracy of the system.

III. IMAGE PROCESSING

This section describes some of the preliminary actions taken for the reference (desired) position image and the actual images taken from the current positions of the camera. The aim of this stage is to find, extract and locate the target pattern.

A. Pattern Selection

The selected pattern is a sketch, which is a combination of three circular patterns which slightly vary in their radii as shown in figure 3. The shown picture is one of the views where the camera is perfectly positioned in lateral directions. The centre of the middle circle in the middle of the image frame is the desired position.

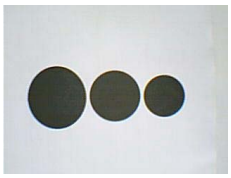

Fig.3. Selected Pattern

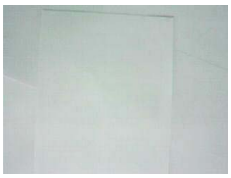

Fig. 4. Background

B. Background Subtraction

One of the background images is shown in figure 4 above. The background is used to be subtracted from the image containing the pattern at each step of radius extraction of the circular patterns. Other steps in the image processing section involve morphological operations, region finding, extraction of the largest circular shape in the image, radius and centre of any black circle and tracking the circular shapes in the image sequence. One of the images where all the circular patterns are tracked is shown in figure 5 below.

C. Position Control

If (x_{rp}, y_{rp}) and (x_{pp}, y_{pp}) are the centers of the desired position and position in the present-time (real-time) of the middle circular pattern in images respectively, then the control actions are taken on the following basis

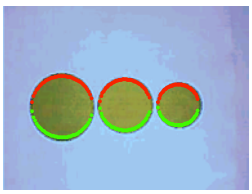

Fig.5. Tracked Circles

The ideal difference should be zero.

$x_{rp} - x_{pp} = 0$; and $y_{rp} - y_{pp} = 0$; .....(1)

We keep some tolerance (errors) to simplify and speed up our system.

Now if the acceptable errors are

$e_{xp} = x_{rp} - x_{pp}$ and $e_{yp} = y_{rp} - y_{pp}$ .....(2)

Then the required conditions are

$$\lim_{t\to\infty}(x_{rp} - x_{pp}) = e_{xp}(t) \text{ and } \lim_{t\to\infty}(y_{rp} - y_{pp}) = e_{yp}(t)$$

.....(3)

The above idea is taken from [8].

IV. DEPTH ESTIMATING CALIBRATION EQUATIONS

The depth estimation calibration equations utilize the image pattern shown in figure 3. Each equation relates the radius of one of the circular patterns in image plane and its corresponding depth of the pattern at that particular position of the camera. Different images were taken from different known depths. The mechanical setup designed for this purpose has two pulleys system such that when the camera moves vertically through one pulley system, the other end moves in the opposite direction of equal amount on a vertical scale attached to the system. For the calibration equations, images of the pattern are taken from five different depths of the camera. The radii of the circular patterns in the image plane are inversely proportional to their corresponding depths, e.g., as the camera come close to the patterns, the radii of the circular patterns will obviously increase in the image. Five different depths were selected from the attached scale and the images were captured in each depth position. A simple algorithm is then applied to find the radii of three circular patterns at their corresponding depths. Let H be the vector containing the entries of five known depths $h_1, h_2, ..., h_5$ i.e.,

$$H = (h_1 \quad h_2 \quad h_3 \quad h_4 \quad h_5) \text{.....(4)}$$

R is the vector of the radii of the three circular patterns

$$R = (r_1 \quad r_2 \quad r_3) \text{.....(5)}$$

The values of the radius r_1 of the largest circular pattern at depths $h_1, h_2, ..., h_5$ can respectively be

$$r_1 = (r_{11} \quad r_{12} \quad r_{13} \quad r_{14} \quad r_{15}) \text{.....(6)}$$

Similarly the numerical values of the radii of the middle and smallest circular patterns at above heights are respectively

$$r_2 = (r_{21} \quad r_{22} \quad r_{23} \quad r_{24} \quad r_{25}) \text{.....(7)}$$

and

$$r_3 = (r_{31} \quad r_{32} \quad r_{33} \quad r_{34} \quad r_{35}) \text{.....(8)}$$

After calculating the radii of each circular pattern at different heights three plots were drawn for each vector r_1, r_2 *and* r_3 with respect to H . A MATLAB based commands were used for getting these graphs. Data curve fitting techniques were then applied to find accurate estimate equations that best fit the drawn plots. In each case it was observed that three-degree polynomials (cubic) best fit the curves. If the H_1, H_2 *and* H_3 are the corresponding depths relating to radii r_1, r_2 *and* r_3 respectively through the three-degree polynomial equations then we have,

$$H_3 = a_1 r_1^3 + b_1 r_1^2 + c_1 r_3 + d_1 \text{.....(9)}$$

$$H_2 = a_2 r_2^3 + b_2 r_2^2 + c_2 r_2 + d_2 \text{.....(10)}$$

and

$$H_3 = a_3 r_3^3 + b_3 r_3^2 + c_3 r_3 + d_3 \text{.....(11)}$$

respectively.

Now the three depths calculated from different circular patterns are then averaged to find a more accurate depth of the camera with respect to the pattern.

$$Depth = (H_1 + H_2 + H_3)/3 \quad \text{.....(12)}$$

V. SIMULATION / EXPERIMENTAL RESULTS

A series of computer simulations and practical experiments were carried out. We ran the MATLAB based algorithm many times and observed the behaviour of the system in response to different commands produced by the software. The output of the USB I/O card was not compatible with the three-channel transmitter system, so for properly interfacing we added interfacing electronics. During the development of the software we faced several problems in the overall control process, but we were making changes continuously and finally we achieved a stable operation of the system. After stabilizing the system, we performed many experiments and stored the results. The procedure of each experiment was as follows.

The first challenge in the design was the proper position of the camera with respect to the geometrical pattern consisting of three circles. The desired position is selected such that the centre of the middle circle comes in the middle of the image frame with some tolerance. The camera was initially displaced at the height of 72 cm from the plane on which the pattern is designed. Real-time images are taken and the centre of the circular pattern is updated each time. Based on the difference between the reference centre point and the ones obtained by image processing of real-times image, the camera is moved to the new position to minimize the error between the two. A pictorial view showing the convergence of the centre point towards the desired one is shown in Fig. 6. The corresponding errors in *x and y* coordinates and its convergence to the selected threshold errors with time are shown below in Figs. 7 and 8 respectively. The error is minimized purely through camera's watch and move technique.

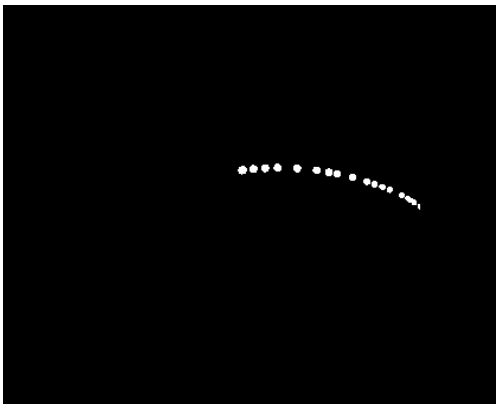

Fig. 6. Flow of position-pattern in position mode

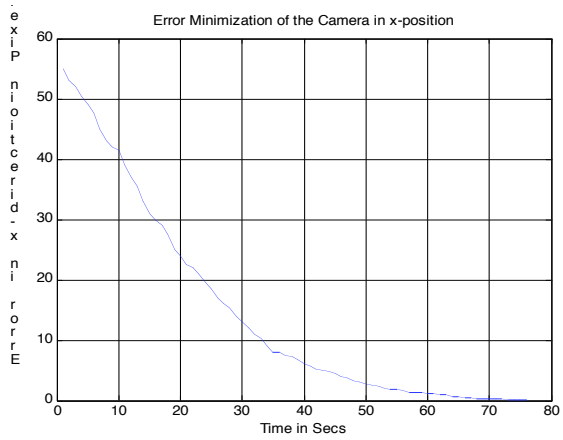

Fig. 7 Error Minimization in x-position

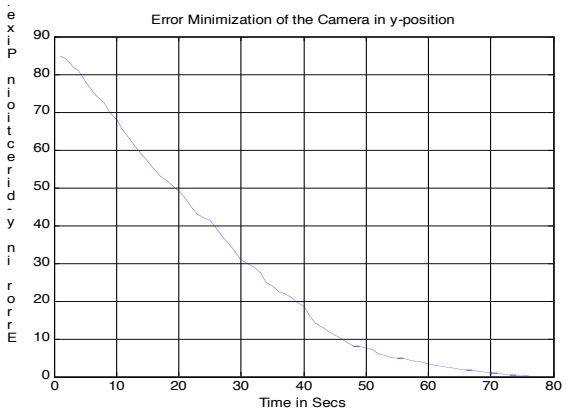

Fig. 8 Error Minimization of camera in y-position

For the depth control mode, the relation between height and radios of the circular pattern in images is obtained from calibration (observation) equations described in section 4. Different heights of the camera from the designed pattern were selected. The heights (in cm) used were by putting values in equation (4).

$$H = (72 \quad 62 \quad 52 \quad 42 \quad 32) \quad \text{.....(13)}$$

A simple algorithm is then applied to the images at the above heights and the radii of the three circular patterns were calculated in each captured image. The three vectors obtained from the radii of the circles of largest, middle and smallest circles were extracted and by putting the values in equations (6), (7) and (8) respectively, we have

$$r_1 = (18.5 \quad 22.5 \quad 27.5 \quad 34 \quad 42) \quad \text{.....(14)}$$

$$r_2 = (16.31 \quad 19 \quad 22.5 \quad 28.5 \quad 35.5) \quad \text{.....(15)}$$

and

$$r_3 = (11.61 \quad 15.5 \quad 19 \quad 23 \quad 29) \quad \text{.....(16)}$$

H is then plotted against each of the r_1, r_2 *and* r_3 and by curve fitting technique, the most suitable fitting (cubic) were selected. The corresponding curves and its best fittings are shown in figures 9, 10 and 11 respectively.

The calibration equations thus found out respectively through largest, middle and smallest circle are calculated by putting values of constant coefficients $a's, b's, c's$ *and* $d's$ in equations (9), (10) and (11).

$$H_1 = -0.00034r_1^3 + 0.059r_1^2 - 4.2r_1 + 130 \quad \text{.....(17)}$$

$$H_2 = -0.0041r_2^3 + 0.39r_2^2 - 14r_2 + 210 \quad \text{.....(18)}$$

and

$$H_3 = 0.0046r_3^3 - 0.23r_3^2 + 1.2r_3 + 83 \quad \text{.....(19)}$$

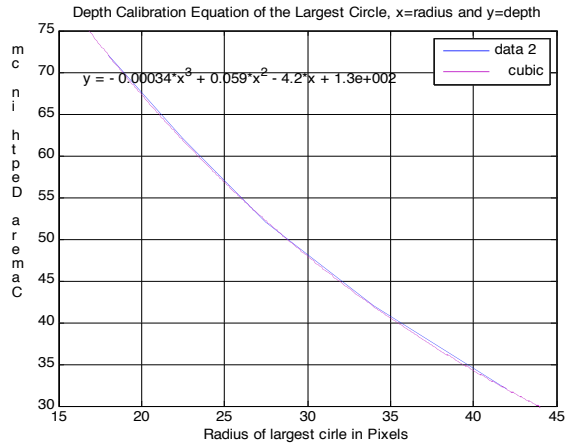

Fig. 9 Curve Fitting of Height Against Radius r_1

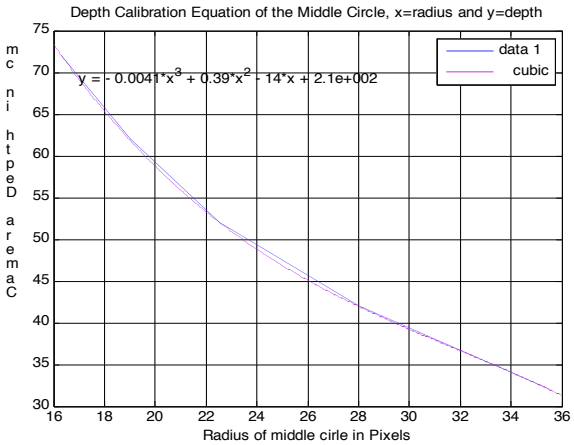

Fig. 10 Curve Fitting of Height Against Radius r_2

The effect of three estimated depth values is then combined to find a more accurate estimation of depth. Equation (12) is applied for this purpose. The estimation of depths calculated are very accurate having accuracy of less than $\pm 0.6cm$ .The true and calculated values of depths are given in table I below with their absolute errors.

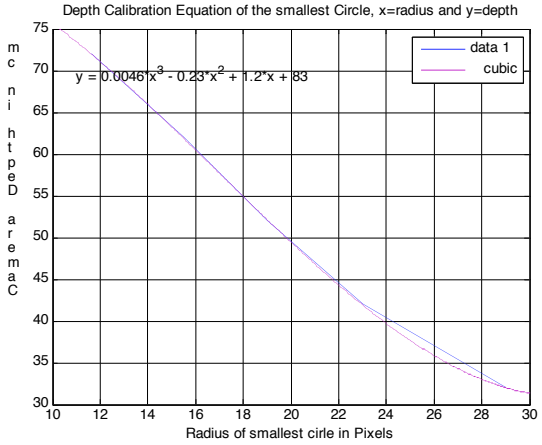

Fig. 11 Curve Fitting of Height Against Radius r_3

TABLE I

True Depth (cm)	Calculated Depth (cm)	Abs. Error (cm)
70	70.1893	0.1893
65	64.9848	0.0152
60	59.4413	0.5587
55	55.3836	0.3836
50	50.5029	0.5029
45	45.3851	0.3851
40	40.3505	0.3505
35	35.4221	0.4221
30	30.5354	0.5354
25	25.4316	0.4316
20	20.3412	0.3412
15	15.2659	0.2659

VI. CONCLUSION AND FUTURE TRENDS

So far this paper is concerned we have worked out to design and implement a real-time vision-based position and depth control of the pattern with respect to camera. The strategy implemented here is independent of the conventional camera calibration containing translation and rotation matrices or extrinsic and intrinsic parameters. Due to simple mathematical equations, the design algorithm is too fast and so is practically applicable to real-time applications. We have added several assumptions, such that the target is stationary and places on a planer surface.

Now we have planned our future strategies to work out some other issues to modify our present design. In future we will work out to minimize the assumptions made in this paper and will make the target (the reference pattern) also movable. Finally we will proceed to work on tracking an unmanned helicopter for precise landing applicable to most of the real time problems.

REFERENCES

[1] S. Saripalli, S. Gaurav, J. F. Sukhatme and J. F. Montgomery, "Vision-based autonomous landing of an unmanned aerial vehicle," In *IEEE international conference on robotics and automation,* Washington D.C., May 2002, pp2799-2804.

[2] A.Q.Khan and Naeem Iqbal, "Modeling and Design of an Optimal regulator for three degree of freedom Helicopter", *IEEE SCONEST* 2004, December 29-31, Karachi.

[3] R. C. Gonzales and R. E. Woods, "Digital Image Processing", Second Edition, Dorling Kindersley (India) Pvt. Ltd, 2002.

[4] R. C. Gonzales, R. E. Woods and S. L. Eddin, *Digital Image Processing Using MATLAB*, Prentice Hall, First Edition, September 2003.

[5] A.Q.Khan, G. Mustafa and N. Iqbal, "LQG/LTR Based Controller Design for Three Degree of Freedom Helicopter/Twin Rotor Control system," in *Proceedings of IEEE-INMIC* 2005, Karachi.

[6] I. Cohen and G. Medioni, "Detection and Tracking of Objects in Airborne Video Imagery," In CVPR 98.

[7] B. Jung and G. Sukhatme, "Detecting moving objects using a single camera on a mobile robot in an outdoor environment," In *international conference on intelligent autonomous systems,* March 2004.